Using Microgap Chambers as a Self Contained Trigger in DØ for TeV33

Gordon Watts[1] and Marvin Johnson[2]
[1] *Brown University, Providence, RI 02912,*
[2] *Fermi National Accelerator Laboratory, Batavia Il., 60510*

ABSTRACT

A Microgap Chamber (MGC) detector is proposed for the DØ detector operating at the Tevatron in luminosities of $\mathcal{L} = 1 \times 10^{33}$ cm^{-2}s^{-1}; the TeV33 era. The detector is made up of pixels, segmented finely in ϕ and coarsely in z. Deadtimeless trigger electronics are mounted directly on the detector to reduce the bandwidth requirements out of the device. Trigger rates and background rejection are estimated with a simulation using single tracks with a fixed P_T and minbias events generated by the DTUJET generator. The Trigger rate and the background rejection are estimated for various strip efficiencies, luminosities, detector noise hit rates, and other parameters. The simulation predicts a MGC based detector is capable of giving the required rejection for a luminosity of 1×10^{33} cm^{-2}s^{-1}.

I. INTRODUCTION

The luminosities of the Fermilab TeV33 proposal are a boon for physics [1]; however they present significant challenges for the detectors. Arguably, the toughest problem is bringing the trigger rates down to manageable levels in the high luminosity environment. Table I lists the luminosities and the expected number of minbias interactions per crossing at the end of Run II and in the TeV33 era [1].

At the peak luminosity of $\mathcal{L} = 2 \times 10^{33}$ cm^{-2}s^{-1}, there will be $\bar{n}= 18$ minbias interactions at every crossing. Simulations show that the DØ Run II fiber tracker's inner layer occupancy will be in excess of 20%; it is impossible for the trigger to operate effectively with such high occupancy [2].

	108 bunches	36 bunches
Peak $\mathcal{L}$	2×10^{33}	1×10^{32}
Peak $\bar{n}$	18	3
Bunch Spacing (ns)	132	396

Table I: The accelerator parameters for the TeV33 project discussed at Snowmass. Luminosity leveling, filling the abort caps, etc. are not considered in this table [3]. Accelerator improvements to bring it to TeV33 luminosities will be gradual. It is expected that the 108 bunches per beam will be reached by the end of Run II.

Both the Run II collider detectors, CDF and DØ, have a three level event trigger. DØ's design handles a 10 kHz Level 1 accept rate, and a 1000 Hz Level 2 accept rate. Level 3, a CPU farm that makes the final decision, has an accept rate of 20 Hz. CDF's bandwidths are similar, however the Level 1 accept rate is much higher to accommodate their $b \rightarrow \pi\pi$ trigger. Beam crossings occur at the rate of 5 MHz with 108 bunches. The Level 1 trigger must have a rejection factor of 500 to keep the rate of Level 1 accepts reasonable. DØ's Run II tracking trigger does not have the required rejection at high luminosities.

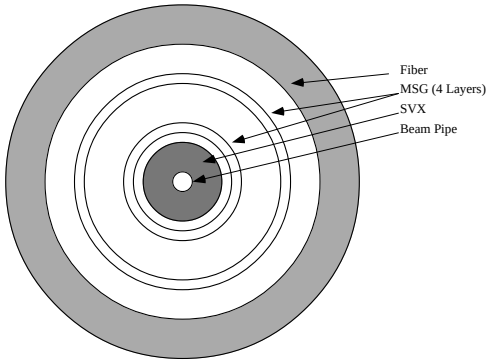

Figure 1: A Possible configuration for the inner tracking volume at DØ with Microgap Chambers (MGCs). The silicon is the inner most detector; there is little mass between it and the interaction point. Room is made between the outer detector and the silicon detector for a MGC detector. For this study we used MGC layers at 20 cm, 22 cm, 30 cm, and 32 cm.

There are two general approaches to reducing the Level 1 accept rate. First, the accelerator may employ tricks to keep the instantaneous luminosity low, thereby keeping $\bar{n}$ small. Second, the detectors that do the triggering can be improved or replaced. A good overview of all the options, including the one discussed in this note, can be found in the TeV33 detector working group report [3]. Possible improvements to the fiber tracker are discussed in a second snowmass report [2].

A pixel detector capable of triggering will improve the rejection substantially. The difficulty with detectors like DØ's Run II fiber tracker is that the occupancy is too high. Each fiber in the Run II fiber tracker is over 2 meters long; unless the detector has very fine ϕ resolution, trigger algorithms will be overwhelmed by combinatorics. A pixel detector, on the other hand, has the opportunity to greatly reduce the number of considered combinations by segmenting both in ϕ and z.

Two options were considered for DØ's inner tracking volume. The inner layers of the silicon detector could be replaced with silicon pixels, 50 μm square. Or, Microgap Chambers (MGCs) – formerly called Microstrip Gas Chambers – could be installed between a silicon detector and an outer detector (such as a modified fiber tracker). A possible inner tracking volume configuration is shown in Figure 1. While this study was carried out with DØ in mind, we expect the results could be applied equally well at other collider detector facilities.

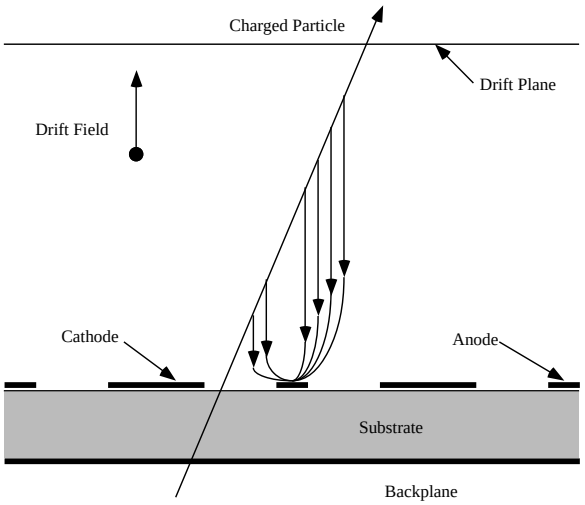

Figure 2: A schematic diagram of MGC operation. A particle passing through the detector leaves a trail of ionized particles which are collected, by the high electric field, on the anodes.

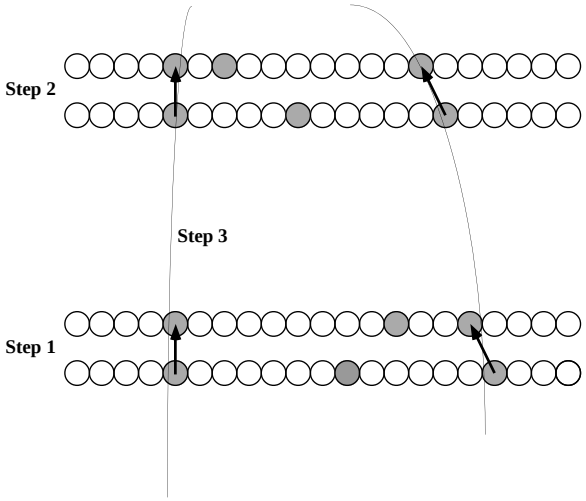

Figure 3: A graphical representation of the triggering algorithm. In step 1 and step 2 the trigger algorithm considers only adjacent layers, forming vectors between the two layers (heavy arrows). Hits, like those in the middle, are not considered because the vectors they form represent tracks whose P_T is below the cut. In step 3 the vectors from the two doublet layers are combined if the P_T of the resulting track is above threshold. The right track would not make the cut, for example. Note that the four middle hits were not considered at all at this stage.

II. THE MGC DETECTOR

The MGC is a small, fast, high resolution proportional chamber. Its operation is very similar to small drift chambers, with a drift length of 3 mm. Even with a moderate speed gas (50 μm/ns), it takes electrons less than 60 ns to reach an anode. Such speed is required in TeV33, where interactions will occur every 132 ns.

The anodes can be placed quite close together, as close as 250 microns. This gives the detector excellent ϕ resolution. The anodes are coarsely segmented in z to reduce the detector occupancy. Figure 2 is a cross section of a layer of a MGC detector.

The radiation length of a layer of a MGC detector is very similar to that of a layer of a silicon detector; the copper of the mounted circuits and substrate are the big contributors to the radiation length.

Atlas plans to use MGCs in the LHC environment, and has a substantial amount of literature on the devices [4].

The design of our MGC detector has been optimized for triggering on 10 GeV/c tracks with good rejection of multiple interaction minbias events. The detector has four layers, grouped in two pairs (see Figure 1). While equally spaced layers are better for offline tracking resolution, moving the inner and outer two layers close to each other forms a powerful trigger by reducing combinatorics.

A. The Trigger Algorithm

The trigger algorithm removes hits from consideration locally to reduce the number of possibilities it must consider globally. The trigger considers each of the two sets of layers individually and then combines the result to form a trigger decision. The pairs of layers are called a "doublet layers".

The trigger algorithm is described pictorially in Figure 3. First, vectors are formed in each doublet layer. The ϕ resolution of each layer is designed to make a coarse P_T cut. A $P_T = 10$ GeV/c track's ϕ will sweep through 132 μm between a layer at $r = 20$ cm and $r = 22$ cm in a 2 Tesla magnetic field. It will sweep through 600 μm between $r = 20$ cm and $r = 30$ cm.

Once doublets are formed, they are combined by projecting the doublet from the inner layer doublet to the outer layer doublet and requiring the resulting track to have $P_T > 10$ GeV/c. The device triggers if an inner-outer doublet satisfies the P_T cut.

The high luminosity environment of TeV33 precludes relying on just four $r - \phi$ layers; the occupancy is too high. To reduce the combinatorics, the detector is segmented in z. Our initial estimate was a strip length of 1 cm, which gives good rejection and some possibility for z resolution in offline tracking. A detector 2 meters long, with layers at 20, 22, 30, and 32 cm with 250 μm$\times$1 cm strips will have 5.2 million strips.

A strawman geometry for the MGC detector is shown in Figure 4. Each of the 1600 towers is assembled separately and mounted in a superstructure (not shown). The towers are self contained except for four links to adjacent towers for transferring hit information. Each layer contains SVX like readout chips, with minor modifications for a trigger pickoff. The upper layer of each doublet contains additional logic (perhaps a field programmable gate array) to form doublets with the layer below it, and, finally, the outer most layer contains the extra logic to combine the doublets to form a trigger. The output is a "yes/no" reported to the Level 1 trigger framework.

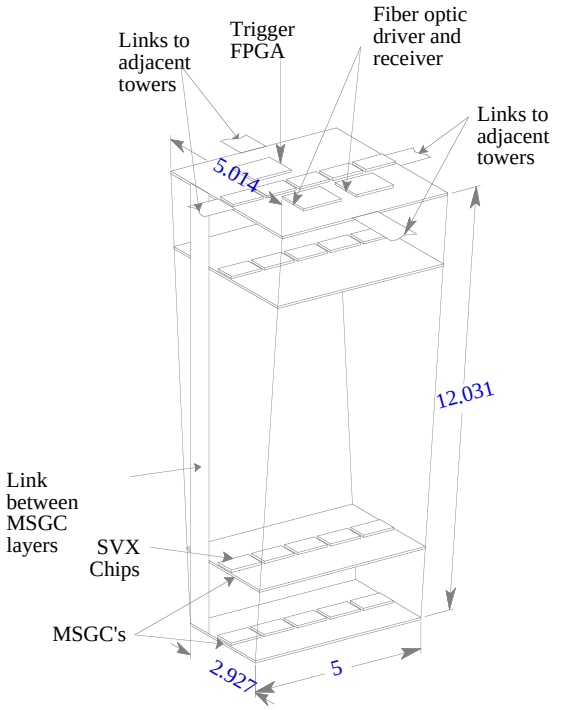

Figure 4: The design of a GMSC tower. A GMSC detector is made up of 1600 of these towers. The lower three layers contain SVXII like read out chips and support to pipe trigger information to the fourth layer. The fourth layer contains enough information to form a trigger in a trigger chip, perhaps an FPGA. The interconnects on the side route information to adjacent modules for tracks that cross boundaries. All units are in cm.

B. Information Flow in the Trigger

Extracting hit information for 5.2 million strips to make a deadtimeless trigger decision for Level 1 is a huge job. Even with a low occupancy of 0.3%, 15,000 strips will be hit each crossing. If each hit is one 32-bit word, that means the data flows out of the detector at a rate of 70 GBytes/sec!

The Run II Level 1 trigger is deadtimeless; the hardware has 3.5 μs to make a decision on a particular crossing, and must have the next crossing's decision 132 ns later.

Further complicating matters is that the inner tracking volume of DØ is already very crowded; it is unlikely that there exists room for the cables needed to support a high speed data link. This leads to the idea of a self triggering device: a local information processor mounted directly on each tower of the detector. The small processors need only examine a fraction of the data.

The trigger algorithm, described above, is similar to the multilevel event triggers used by both CDF and DØ. Each doublet layer examines hits from its two layers, discarding the hits that do not pass the P_T cut. The discarded hits do not have to be passed on to the next phase. Further, only the vector formed from the two hits, and not the two hits themselves, need to be transferred.

Real problems remain to be solved for this algorithm. While a lot of hits are discarded, there is still the problem of information sharing between towers. Little will be shared along the ϕ axis: high P_T tracks do not bend very much. The z axis, however, is another matter.

The simulation will happily form a doublet layer vector using two hits very close together in ϕ at opposite ends of the detector. Of course, the doublet will never form a trigger because it never intersects with the other doublet layer, however, the information has to travel from one end of the detector down to the other in 132 ns. High luminosity simulations predict over 400 doublet vectors on each of the two doublet layers. To reduce the number of formed doublet vectors one can impose cuts on the angle of the track: if it comes from too far outside the central region don't transmit the information.

A possible hardware solution is to limit the length of the bus in the z direction carrying the hit information. Two sets of buses walk the length of the detector. Each bus in a set is long enough to get a hit located at one end of the bus as far as required to cover all possible doublet vectors that satisfy the angle cut. One of set of buses is offset by half a bus length from the other. All hits are allowed to jump one bus; thus no hit is more than two buses away from a possible partner.

III. SIMULATION

A simulation was written during the Snowmass conference and further worked on during the summer. The simulation was written on a PC running Windows NT. It is written in C++, and thus is quite transportable (it ran with minor modifications on both a UNIX box and a Apple Mac). Output is both text and VRML (Virtual Reality Modeling Language) [5]. Netscape is used to view the VRML output in 3D. The 3D output proved very useful tracking bugs in the track finding algorithm.

Minbias events are generated using DTUJET [6]. Significant work by both DØ and CDF means we can expect DTUJET to generate the correct track multiplicities and P_T spectra. 6000 events were generated. The number of minbias interactions to be combined for each simulated event is determined with a poisson distribution of mean $\bar{n}$. The individual minbias events are rotated randomly in ϕ, and their z vertex is given a gausian distribution of width 20 cm[1].

Each charged particle is propagated through the MGC. No multiple scattering, absorption, or decay is simulated. The detectors are assumed to have no thickness in r (no charge sharing or double hits due to a particle passing through at large angles), and there are assumed to be no gaps in the geometry. The number of hits to be added per layer is determined by a gausian distribution with a mean of 11.3 hits per minbias interaction. There is no noise component that is luminosity independent.

The trigger algorithm does not have roads, per se, as do other track finding algorithms. There are two tunable parameters that control the doublet vector creation and the matching of vectors between the two doublet layers.

A simple search over the parameter space is performed, optimizing the quantity signal squared over background. The P_T distribution of tracks from minbias events show there are few tracks above 8 GeV/c. In the 6000 minbias events, there are only 6 tracks with $P_T > 8$ GeV/c. We choose single tracks with $P_T = 8$ GeV/c to measure the background rate. The trigger threshold is 10 GeV/c, and $P_T = 10$ GeV/c tracks are used to measure the signal rate. It would be more accurate to tune, for background, using the simulated minbias events. However, the CPU time requirements are prohibitive. There is some evidence that tuning by hand may be able to get slightly better results.

A. Results

There is a huge parameter space to explore; there is not room to report all of it here. The detector configuration that proved optimal is shown in Table II. The turn-on curve for the trigger, shown in Figure 5, was determined by looking at 10,000 tracks at each energy point. Figure 6 shows the trigger rejection as a function of luminosity.

QCD dijet events will cause a trigger if they contain tracks with high enough P_T. A study using ISAJET shows that QCD prevents the trigger rejection from ever getting better than a factor of 700 at $\mathcal{L} = 10 \times 10^{32}$ cm^{-2}s^{-1} and 350 at $\mathcal{L} = 20 \times 10^{32}$ cm^{-2}s^{-1}; as the trigger finds real tracks. These limits are depicted as the two points in Figure 6. Rejection better than this limit will not be realized at Level 1 unless information from other detectors is combined with the track trigger information (*i.e.* the calorimeter).

The reason a MGC has good rejection is that its occupancy is low, which reduces the possibility of several different tracks fooling the trigger into finding a single track above threshold. Occupancies of the four layers are shown in Table III for simulations at $\mathcal{L} = 10 \times 10^{32}$ cm^{-2}s^{-1} and $\mathcal{L} = 20 \times 10^{32}$ cm^{-2}s^{-1}.

[1]In TeV33, the p and $\bar{p}$ beams are expected to have a crossing angle which keeps the interaction region small.

Parameter	Layer 1	2	3	4
Radius (cm)	20.0	22.0	30.0	32.0
ϕ pad size (μm)	250	250	250	250
z pad size (cm)	1.0	1.0	1.0	1.0
Pixels (millions)	1.00	1.11	1.51	1.61

Table II: The configuration of the detector that had the best S^2/B. Projective geometry would call for larger ϕ sizes on the outer layers, however, a slightly better trigger rate was observed for this configuration.

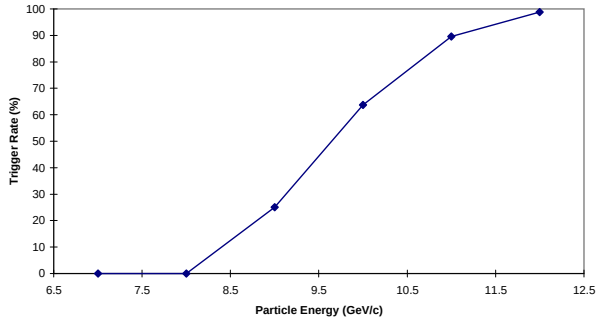

Figure 5: The turn on curve for the trigger. Single particles with random charge and a set P_T are propagated through the detector to determine the turn on curve.

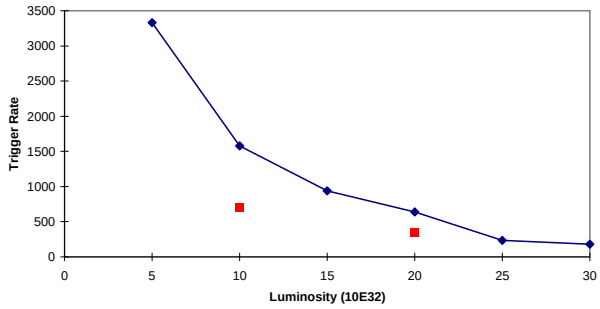

Figure 6: The trigger rate as a function of luminosity for the best detector configuration. The QCD dijet cross section will produce jets that contain $P_T > 10$ GeV/c tracks. QCD processes are expected to generate triggers that make reducing the actual rejection below the solid squares difficult.

	Occupancy	
Layer	10×10^{32} cm^{-2}s^{-1}	20×20^{32} cm^{-2}s^{-1}
1	0.31%	0.62%
2	0.28%	0.56%
3	0.17%	0.34%
4	0.15%	0.30%

Table III: The occupancies for the four layers of the detector (layer 1 is the inner most layer) at two luminosities. Noise was included in this calculation.

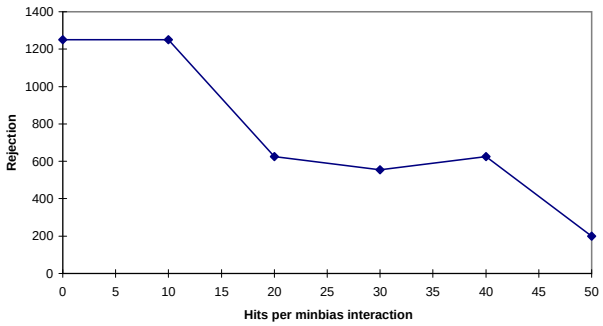

Figure 7: The trigger rejection as a function of the hits per layer per minbias interaction added to simulate noise. The luminosity for this simulation is 10×10^{32}. The nominal number is 11.3.

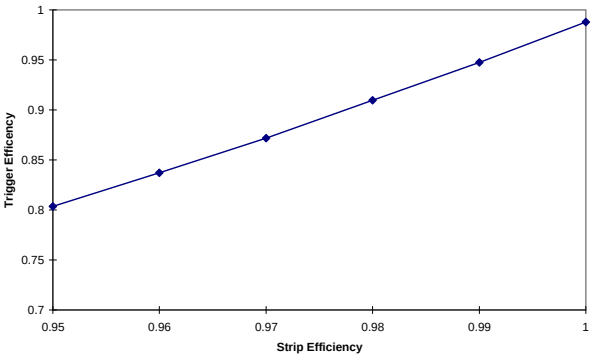

Figure 8: The trigger rate as a function of GMSC strip efficiency. This trigger requires that there be a hit on all four layers.

The trigger's rejection is only mildly susceptible to noise. Figure 7 shows the trigger's rejection as a function of the number of hits added per layer per minbias interaction. Even at four times the nominal noise rate, the trigger performs well.

The trigger algorithm requires all four layers to have a hit from the track. The MGCs are not, of course, 100% efficient. Figure 8 shows that the trigger rate degrades quickly as the strip efficiency falls off. Test detectors have achieved 98% efficiency [7].

IV. OTHER STUDIES

There is reason to believe that the rejection can be improved. Of 8 events out of 10,000 that pass for a simulation at $\mathcal{L} = 10 \times 10^{32}$ cm^{-2}s^{-1}, four are due to a single 8 GeV/c track, and the other four are due to noise hits combined with hits from several low P_T tracks. Good z information could further reduce these accidentals. However, unless the QCD background is reduced, the improvements will only be for the satisfaction of having a perfect (if impractical) trigger.

The focus of the snowmass study was MGCs as a stand-alone triggering device. Very little attention was paid to how it would fit into the overall tracking environment. While it is easy to imagine that an outer fiber tracker would provide excellent P_T resolution through its lever arm and good z resolution with its stereo strips, and that an inner silicon detector would provide a good beam constraint for a track fit, much work remains before this can be accomplished. Because a pixel-like device has some z resolution, it may be instrumental in track pattern recognition and linking the inner tracker with little or no z resolution and an outer tracking detectors with good z resolution.

The MGC trigger algorithm depends on the beam traveling along the central axis of the detector. While this will be close to true, the beam will move from store to store. CDF, which plans to use their SVX in their Run II Level 2 trigger, requires active alignment (on a store-by-store basis) of the SVX to keep the trigger efficient. The MGCs are unlikely to require anything that complex, but their performance will degrade as the beam moves off center.

V. CONCLUSION

The MGC technology is promising. With other experiments, like Atlas, committed to the technology, it seems likely that it will be available on the timescale required for Run II. The idea of a self triggering device also makes the MGC detector discussed very attractive: the Level 1 triggering hardware is small and built into the detector.

The simulation predicts the MGCs achieve rejection better than the predicted QCD background rate. The MGC performs as well as it does with the light weight triggering hardware and small number of layers because of its fine segmentation in ϕ and z.

This work is supported in part by U.S. Department of Energy Grant DE-FG02-91ER40688.

VI. REFERENCES

[1] *TeV-2000 Group Report*, D. Amidei and R. Brock, editors. 1996. `http://www.pa.msu.edu:80/hep/tev2000/`
Report of the Tev33 Committee, J. Appel *et al*, `http://www-theory.fnal.gov/tev33.ps`

[2] *Upgrading the DØ fiber tracker for TeV33*, Rich Partridge *et. al.*, Snowmass '96 proceedings.

[3] *Report of the TeV33 Detector Working Group*, F. O. Borcherding *et. al.*, Snowmass '96 proceedings.

[4] *Many Atlas Inner Detector Notes* `http://atlasinfo.cern.ch/Atlas/GROUPS/INNER_DETECTOR/NOTES/notes.html`.

[5] *The VRML Sourcebook* Andrea L. Ames, David R. Nadeau, and John L. Moreland. Wiley, 1996.

[6] P. Aurenche, *et al*, Phys. Rev. **D45** (1992) 92. See also, F.W. Bopp, *et al*, Z. Phys. **C51** (1991) 99.

[7] *Talk to the TeV33 Working Group at Snowmass'96* S. Kwan, Fermilab